The current issue and full text archive of this journal is available on Emerald Insight at:
www.emeraldinsight.com/0332-1649.htm

Artefact reduction in fast Bayesian inversion in electrical tomography

Hubert Zangl and Stephan Mühlbacher-Karrer
Institute of Smart System Technologies, Sensors and Actuators Group, Alpen Adria Universität, Klagenfurt, Austria

Received 25 February 2015
Revised 27 April 2015
Accepted 28 April 2015

Abstract

Purpose – The purpose of this paper is to reduce the artifacts in fast Bayesian reconstruction images in electrical tomography. This is in particular important with respect to object detection in electrical tomography applications.

Design/methodology/approach – The authors suggest to apply the Box-Cox transformation in Bayesian linear minimum mean square error (BMMSE) reconstruction to better accommodate the non-linear relation between the capacitance matrix and the permittivity distribution. The authors compare the results of the original algorithm with the modified algorithm and with the ground truth in both, simulation and experiments.

Findings – The results show a reduction of 50 percent of the mean square error caused by artifacts in low permittivity regions. Furthermore, the algorithm does not increase the computational complexity significantly such that the hard real time constraints can still be met. The authors demonstrate that the algorithm also works with limited observations angles. This allows for object detection in real time, e.g., in robot collision avoidance.

Originality/value – This paper shows that the extension of BMMSE by applying the Box-Cox transformation leads to a significant improvement of the quality of the reconstruction image while hard real time constraints are still met.

Keywords BMMSE, Box-Cox, ECT, OFOA, OSOA, Real time

Paper type Research paper

I. Introduction

Electrical capacitance tomography (ECT) is a well-investigated and well-documented method to non-invasively determine the permittivity distribution in a pipe and to provide cross-sectional images of this distribution. The permittivity distribution within a region of interest (ROI) is reconstructed from measurements of the electrical capacitances between sets of electrodes, e.g. placed on the outer circumference of a non-conductive pipe section or on the surface of an object to monitor its surroundings (e.g. Plaskowski *et al.*, 1995; Isaksen, 1996; and Yang and Peng, 2003).

This procedure leads to a non-linear and ill-posed inverse problem, where the number of unknowns (i.e. pixel number) typically exceeds the number of independent measurements (i.e. different pairs of electrodes). The reconstruction methods require some kind of regularization (e.g. Tikhonov regularization, total variation) in order to provide a reasonable solution.

This work was partially funded by the Austrian Science Fund (FWF) through the project P21855, SafeTom: Safety by Electrical Capacitance Tomography.

COMPEL: The International Journal for Computation and Mathematics in Electrical and Electronic Engineering
Vol. 34 No. 5, 2015
pp. 1381-1391
Emerald Group Publishing Limited
0332-1649
DOI 10.1108/COMPEL-02-2015-0094

In our research, we aim to use the images obtained with electrical tomography to detect objects (e.g. Schlegl *et al.*, 2013). We use this in robotic applications, e.g. collision avoidance for human safety (Figure 1) or in robot graspers. This implies two requirements:

- The algorithms need to work in real time, i.e. we have less than one millisecond in collision avoidance for data acquisition, reconstruction, decision and execution (i.e. more than 1,000 frames per second). The signal processing hardware may comprise comparatively slow low power microcontrollers.
- Artifacts, i.e. ghost images at locations where no object is present, should not appear in the image.

Low complexity reconstruction is typically achieved with non-iterative algorithms such as linear backprojection (LBP), offline iteration/online reconstruction (OIOR) or fast Bayesian methods (Bayesian linear Minimum Mean Square Error (BMMSE)) such as optimal first/second-order approximation (OFOA, OSOA). Also approaches based on neural networks as suggested for electrical impedance tomography Adler and Guardo (1994) and Jeon *et al.* (2005) and also for capacitance tomography Nooralahiyan *et al.* (1995) and Zang *et al.* (2006) may be suitable for resource limited systems and implemented, e.g. in an FPGA. Other approaches in the field of electrical impedance tomography using reduced-order modeling achieve frame rates in the order of 500 frames per second on a quad core computer (Voutilainen *et al.*, 2012). In this paper, we further investigate the Bayesian approach as it combines reasonable and predictable reconstruction quality with low computational effort. While the overall reconstruction performance of fast Bayesian algorithms such as OSOA can be quite good it was found that artifacts may occur in regions where the permittivity is low. This is not too surprising as the influence of the material on the measurements is strongly non-linear, whereas the algorithm is constraint to linear or quadratic functions of the measurements. Consequently, it appears to be feasible to perform a non-linear transformation, e.g. the Box-Cox transformation Box and Cox (1964), of the permittivity and apply fast BMMSE algorithms to the transformed values to be able to meet the requirements in robotic applications.

The paper is structured as follows. In Section II, we describe the fast Bayesian approach. In Section III, we present a concept to reduce artifacts of these algorithms by using the Box-Cox transform and show simulation results. In Section IV, we present experimental results focusing on object detection with limited observation angle and we summarize our results in Section V.

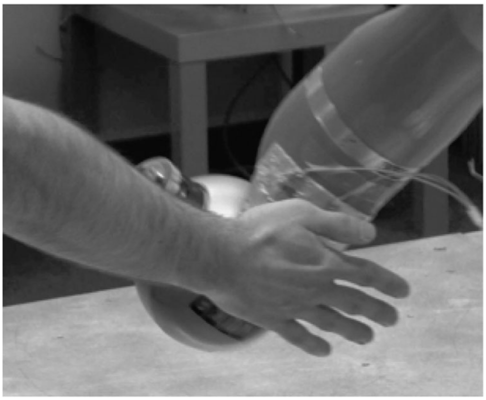

Figure 1.
Example application of Electrical Capacitance Tomography for robot collision avoidance Schlegl *et al.* (2013)

II. Fast Bayesian reconstruction

The means square error between the reconstruction result and the true spatial permittivity distribution is given by:

$$\mathrm{MSE} = \mathrm{tr}\left\{E\left\{(\hat{\varepsilon}-\varepsilon)(\hat{\varepsilon}-\varepsilon)^T\right\}\right\} = \sum_{i=1}^{N} e_i^2 \tag{1}$$

where $E\{.\}$ represents the expectation and ε is a random vector representing the spatial distribution of the permittivity observed at locations of interest and $\hat{\varepsilon}$ the corresponding estimator (reconstruction result), $tr\{.\}$ is the trace of a matrix. However, the reconstruction result $\hat{\varepsilon}$ is obtained from the measurement data $\mathbf{y}$ (with $\mathbf{y}$ being a realization of the random vector $\mathbf{Y}$)[1]:

$$\hat{\varepsilon} = f(\mathrm{y}) \tag{2}$$

which depends on the true spatial permittivity distribution ε and in turn it is a random vector due to measurement noise and other random deviations. In case of additive noise this is given by:

$$\mathbf{Y} = g(\varepsilon)+\mathbf{N} \tag{3}$$

where $\mathbf{N}$ is the random noise vector, e.g. following a jointly Gaussian distribution. The function g(.) represents the forward problem and can be calculated, e.g. using finite element simulations.

In order to find the optimal reconstruction function we have to minimize the expected value of the mean square error *MSE* between the reconstruction result obtained by the function *fi* and the true permittivity value ε_i by:

$$f_{i,opt} = \arg\min_{f_i \in \Phi} E\left\{(f_i(\mathbf{Y})-\varepsilon_i)^2\right\} = \arg\min_{\mathrm{f}_i \in \Phi} E\left\{(f_i(g(\varepsilon)+\mathbf{N})-\varepsilon_i)^2\right\} \tag{4}$$

where $\mathrm{f}_{i,opt}$ is the optimal reconstruction function for the *i*th reconstruction element out of the set of allowed reconstruction functions $\mathbf{\Phi}$. Please note that the optimization could be done for each reconstruction element independently. However, the prior distribution for all reconstruction elements has to be known.

The expected value of the permittivity conditioned on the measurement (posterior distribution):

$$\hat{\varepsilon}_{\mathrm{MMSE}} = E\ \{\varepsilon|\mathbf{y}\} \tag{5}$$

is – with no constraints on $\mathbf{\Phi}$ – a solution of (4) and thus becomes an optimal estimator to minimize the mean square error.

The posterior probability distribution needed to evaluate (5) can be obtained using Bayes' rule (e.g. Kay, 1993):

$$p(\varepsilon|\mathbf{y}) = \frac{p(\mathbf{y}|\varepsilon)p(\varepsilon)}{p(\mathbf{y})} \tag{6}$$

In order to apply (6) we need the prior distribution of the permittivities. In Watzenig and Fox (2009) the authors summarize common choices for the prior and describe the evaluation of (6) by means of Markov Chain Monte Carlo (MCMC) methods. Certain variants have been suggested, e.g. in Bardsley (2012) also for linear models. Although methods like MCMC provide fairly optimal solutions, their computational complexity makes them less attractive for real time reconstruction on resource constraint hardware.

Consequently, we want to speed up the procedure. One approach is to restrict the allowed reconstruction functions to simple functions, e.g. linear functions. This leads to the linear minimum MSE (LMMSE) approach, where we assume that (5) can be approximated by a linear function of the measurement vector:

$$\hat{\varepsilon}_{\mathrm{MMSE}} = W\mathrm{y} + B \approx E\ \{\varepsilon|\mathbf{y}\} \tag{7}$$

It can be shown that the optimal solution is obtained with:

$$W = C_{\varepsilon Y} C_{YY}^{-1} \tag{8}$$

and:

$$B = \overline{\varepsilon} - W\overline{\mathbf{y}} \tag{9}$$

where $C_{\varepsilon Y}$ is the cross-covariance matrix between the measurements and the permittivities and C_{YY} is the auto-covariance matrix of the measurements. The expected value of the permittivity according to the prior probability is denoted by $\overline{\varepsilon}$ and correspondingly the expected value of the measurements by $\overline{\mathbf{y}}$.

This means that all we need to know about the prior distributions are the first two moments of the joint distributions, it is not necessary that the distributions are Gaussian. The first two moments can be found using the sampling technique suggested in Zangl *et al.* (2007), which falls into the category of sample based priors according to Watzenig and Fox (2009). By means of Monte Carlo sampling, samples are drawn from the prior distribution and the covariances matrices are calculated based on a large number of samples. As this is only needed to determine the coefficients of the linear model, a large number of samples can be generated. In Zangl *et al.* (2007) a slightly different notation is used but the result is equivalent to (8) and (9). The approximate optimality (approximate as it is based on random sampling) in the least squares sense is also proven in Zangl *et al.* (2007), therefore we use the term optimal first order approximation (OFOA). When we replace the measurement vector y by an extended measurement vector $\tilde{y}$ that includes the squared measurement values (we thus virtually double the number of measurements):

$$\tilde{y} = \left(y_1, \ldots, y_n, y_1^2, \ldots, y_n^2\right)^T \tag{10}$$

and replace $C_{\varepsilon Y}$ and C_{YY} by $C_{\varepsilon \tilde{Y}}$ and $C_{\tilde{Y}\tilde{Y}}$ accordingly, we obtain what we call optimal second order approximation (OSOA). Therefore, these algorithms are specific/extended implementations of a Bayesian linear minimum mean square estimator meeting real time constraints. Figure 2 illustrates the assumed prior probability distribution of the permittivity by means of a sample, the expected value and the covariance between a selected reconstruction element and all other reconstruction elements. We found that the choice of the prior distribution is not too critical with respect to the performance of the algorithm.

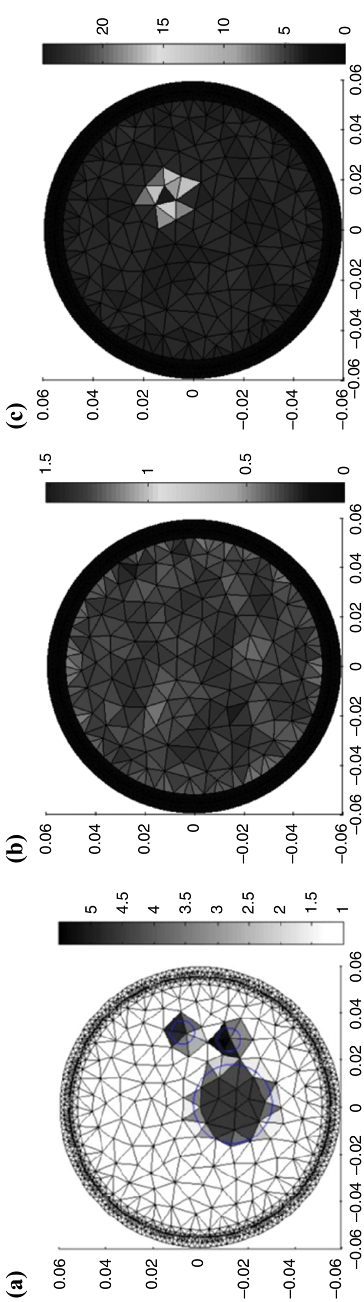

Notes: c, The image shows the covariance of one selected triangle (located at about x = 0:015 m, y = 0:012 m) with all other elements. The strong correlation with neighboring elements can be exploited to reduce the number of reconstruction elements (sparse reconstruction)

Figure 2.
(a) Illustration of a sample drawn from the prior probability distribution of the permittivity distribution ε. Between one to three rods (here: 3) with random, homogeneous permittivity are randomly placed and mapped onto a simulation model (here: 2D Finite Element Model); (b) distribution of the average permittivity as obtained with the described sampling strategy. The expected value for the corresponding prior distribution is fairly homogenous over the entire region of interest. (c) Illustration of the obtained covariance of the permittivities as obtained with the described prior distribution

III. Artifacts and artifact reduction

An example for a reconstruction result for an actual measurement in a traditional ECT configuration is shown in Figure 3. Although the reconstruction is very fast as it requires only a matrix-vector multiplication and thus fulfills the one millisecond requirement, the quality of the reconstruction compares well with other approaches (Zangl *et al.*, 2007).

However, in the given example we observe a ghost image in the upper right part of the region of interest, which can lead to an incorrect object location.

In case that we apply a hypothesis test to detect an object with the hypotheses:

$$\begin{aligned} H_0 &\quad : \text{Object is present} \\ H_1 &\quad : \text{No object is present.} \end{aligned} \tag{11}$$

which corresponds to:

$$\begin{aligned} H_0 &\quad : \varepsilon_i = 1 \ \forall i \in R \\ H_1 &\quad : \exists i \in R \middle| \varepsilon_i > 1 \end{aligned} \tag{12}$$

where R represents the set of indices of elements within the region of interest, we might detect an object in the upper right part that is actually not present. Consequently, applying the Neyman-Person theorem to maximize the detection rate at a given false alarm rate will lead to a rather high threshold and small objects or objects with low permittivity will not be detectable.

As already mentioned the overall reconstruction performance of fast constrained BMMSE can be quite good. However, this comes with the drawback that artifacts may occur in regions with low permittivity due to the strongly non-linear influence of the material on the measurements.

In order to reduce the artifacts, we apply the Box-Cox transform Box and Cox (1964) given by:

$$\varepsilon_i^{(\lambda)} = \begin{cases} \frac{\varepsilon_i^{\lambda}-1}{\lambda} & \lambda \neq 0 \\ \log \varepsilon_i & \lambda = 0 \end{cases} \tag{13}$$

on our permittivity data that we obtain by means of Monte-Carlo sampling from the prior distribution. The parameter is λ is the transformation parameter and allows

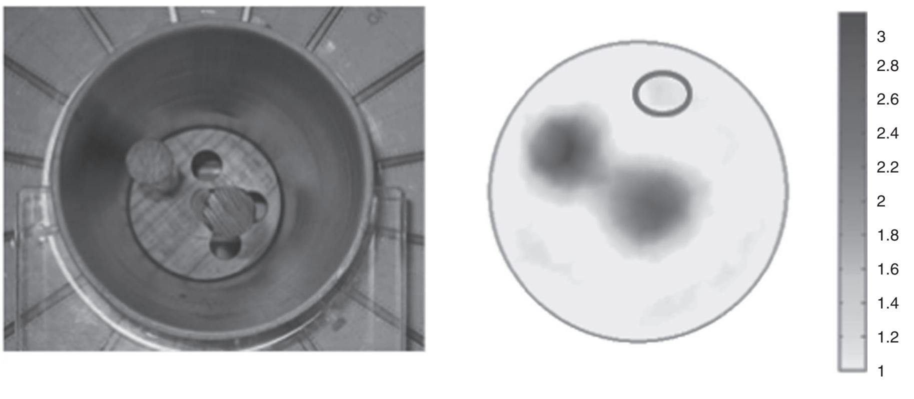

Figure 3.
Comparison of true distribution and reconstruction results using OSOA Zangl *et al.* (2007). The reconstruction time is below 200 μs

realizing different non-linear mappings. Negative values of λ lead to an inverse proportionality whereas positive values to a direct proportionality. Based on our transformed samples we use a grid search approach to find the optimal value for λ by minimizing:

$$\lambda = \arg \min_{\tilde{\lambda} \in \mathfrak{R}} \left(E\left\{ WY + B - \varepsilon^{\tilde{\lambda}} \right\} \right) \quad (14)$$

where ε^{λ} means that the Box-Cox transform is applied to every element of the vector ε as given in (13). We obtained an optimal value of $\lambda = 0.7$ for a setup and a prior distribution as described above.

Figure 4 shows the benefit of the Box-Cox transform based on simulated data. With the transform the mean square error in regions where no object is present is significantly reduced by about 50 percent. Consequently, the hypothesis test according to (12) achieves a significantly better separation using a lower threshold for the permittivity value and thus allows to detect smaller objects or objects with lower permittivity.

IV. Experimental setup and experimental results

In the previous examples we showed configuration according to the classical ECT setup, because it allows to compare the proposed algorithm with well investigated state of the art methods. However, in this section we want to demonstrate that the algorithm also works with limited observation angles and can be applied to object detection problems.

Figure 5 shows a photograph of our experimental setup and an example object. As object a stick with a diameter of $d_s = 20$ mm made of Ertalon with a relative permittivity of $\varepsilon_{r,ertalon} = 3.9$ is used for the experiment. The sensor front end consists of seven electrodes on a planar surface that are connected to an evaluation circuitry by means of coaxial cables. The circuitry generates an AC excitation signals and applies it in sequence to the seven electrodes. The receiver electrodes use low impedance measurement and thus measure the displacement current using I/Q demodulation. The frequency of the excitation signal can be adjusted and was set to 1 MHz in the given example.

Figure 6 shows a sample as obtained during determination of the first two moments of the prior distributions. In this case we use a 3D forward model and calculate g using a commercial solver (COMSOL).

Figure 7 shows the reconstruction result for measurements obtained with the geometry shown in Figure 5. The region of interest is the cross section above the sensor and here we use 101×101 reconstruction elements over $160\,\mathrm{mm} \times 50\,\mathrm{mm}$. As long as objects are not too far from the electrodes, the obtained results are comparable to results for classical ECT.

V. Conclusion

We demonstrate that with the optimal choice of the Box-Cox transformation a reduction of the mean square error in low permittivity regions and thus the artifacts of approximately 50 percent can be achieved while the total mean square error is also reduced. The computational cost of the transformation is only linear in the number of reconstruction elements and number of measurements such that the overall computation time still remains low enough for use in real-time applications. As object detection may directly work on transformed permittivity values, the non-linear Box-Cox transform may not be needed in the real-time reconstruction but only in finding the reconstruction algorithm. We demonstrate that the algorithm even allows to reconstruct images with

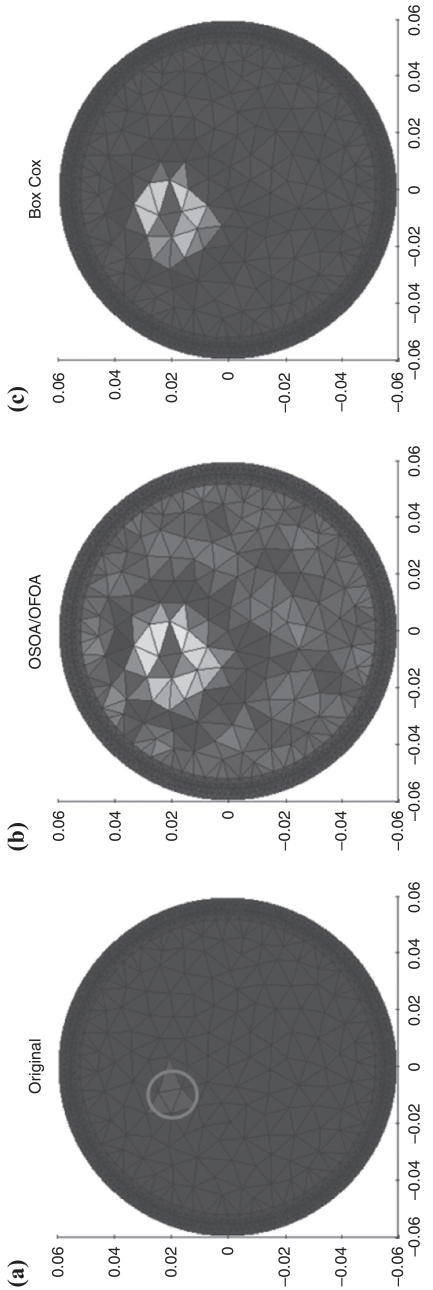

Figure. 4.
(a) Original distribution; (b) reconstruction result using OSOA; (c) reconstruction result using Box-Cox transform. The mean square error in regions where no object is present is reduced by about 50 percent

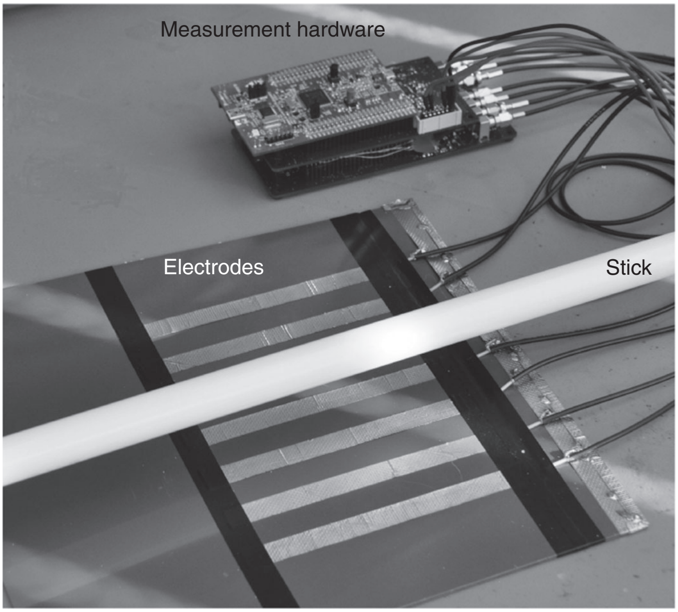

Notes: In contrast to classical ECT, the electrode array does not enclose the region of interest but is instead mounted on a surface. Thus, we obtain only measurements from a quite limited observation angle. Consequently, with increasing distance from the electrodes, the accuracy of the reconstruction decreases Schlegl *et al*. (2013)

Figure 5. Setup of the ECT system for object detection

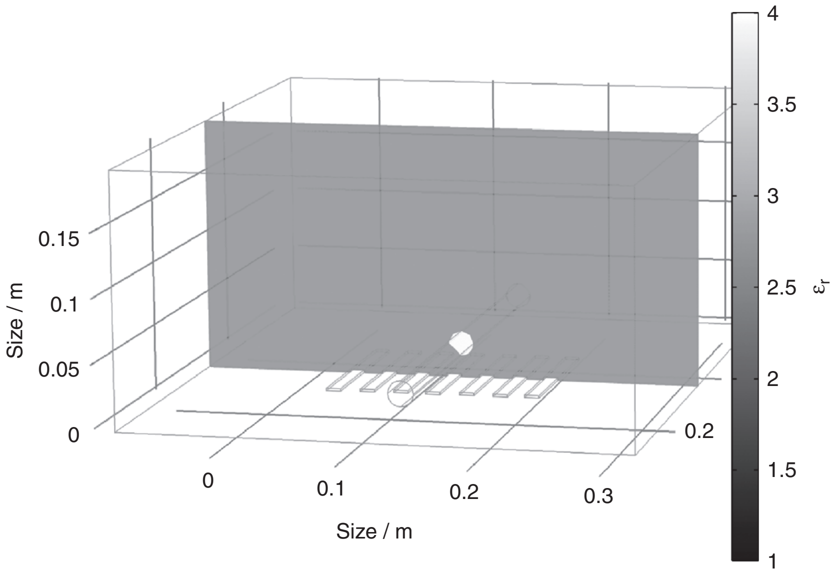

Figure 6. Finite element model of a sample from the prior distribution for the measurement setup according to Figure 5. Here, we use a full 3D forward model to consider leakage effects Zangl and Neumayer (2009) but we reconstruct the cross section as a 2D image

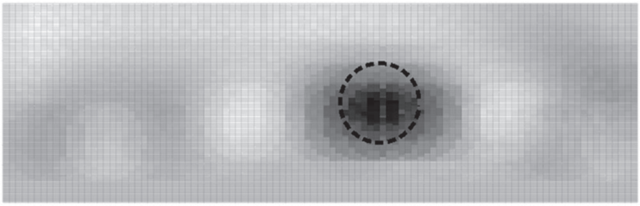

Figure 7. Example of a reconstruction result for measurements obtained with the setup shown in Figure 5

Notes: The electrode array is located at the lower boundary of the rectangle. The region of interest is the cross section above the sensor and here we use 101×101 rectangular reconstruction elements over 160 mm $\times$ 50 mm. The true position of the object ($\varepsilon = 3{:}9$) is illustrated by dashed lines. Although the observation angle is quite limited, the reconstruction result is comparable to classical ECT as long as the object does not reside too far from the electrodes

electrode arrays that do not enclose the region of interest and thus only allow a very limited observation angle. This is in particular useful for object detection, e.g. in robot collision avoidance.

Note

1. Please note that we use ε and $\hat{\varepsilon}$ for both, random vector and realization of true and estimated permittivity distributions in order to avoid confusion by using additional symbols for the permittivity.

References

Adler, A. and Guardo, R. (1994), "A neural network image reconstruction technique for electrical impedance tomography", *IEEE Transactions on Medical Imaging*, Vol. 13 No. 4, pp. 594-600.

Bardsley, J. (2012), "MCMC-based image reconstruction with uncertainty quantification", *SIAM Journal on Scientific Computing*, Vol. 34 No. 3, pp. A1316-A1332, eprint, available at: http://dx.doi.org/10.1137/11085760X

Box, G.E. and Cox, D.R. (1964), "An analysis of transformations", *Journal of the Royal Statistical Society. Series B (Methodological)*, pp. 211-252.

Isaksen, O. (1996), "A review of reconstruction techniques for capacitance tomography", *Measurement Science and Technology*, Vol. 7 No. 3, pp. 325-337.

Jeon, H.J., Kim, J.H., Choi, B.Y., Kim, K.Y., Kim, M.C. and Kim, S. (2005), "Electrical impedance imaging of binary mixtures with boundary estimation approach based on multilayer neural network", *IEEE Sensor Journal*, Vol. 5 No. 2, pp. 313-320.

Kay, S.M. (1993), "Fundamentals of statistical signal processing: estimation theory", Prentice Hall, Upper Saddle River, New Jersey, pp. 379-415.

Nooralahiyan, A.Y., Boyle, B.S. and Bailey, J. (1995), "Performance of neural network in image reconstruction and interpretation for electrical capacitance tomography", *IEE Colloquium on Innovations in Instrumentation for Electrical Tomography*, pp. 5/1-5/3.

Plaskowski, A., Beck, M.S., Thorn, R. and Dyakowski, T. (1995), *Imaging Industrial Flows: Applications of Electrical Process Tomography*, Taylor & Francis, New York.

Schlegl, T. *et al.* (2013), "Virtual whiskers: highly responsive robot collision avoidance", *In: Intelligent Robots and Systems (IROS), 2013 IEEE/RSJ International Conference on*, pp. 5373-5379, doi: 10.1109/IROS.2013.6697134.

Voutilainen, A., Lipponen, A., Savolainen, T., Lehikoinen, A., Vauhkonen, M. and Kaipio, J. (2012), "Fast adaptive 3-d nonstationary electrical impedance tomography based on reduced-order modeling", *IEEE Transactions in Instrumentation and Measurement*, Vol. 61 No. 10, pp. 2665-2681, available at: http://ieeexplore.ieee.org/stamp/stamp. jsp?arnumber=6198416

Watzenig, D. and Fox, C. (2009), "A review of statistical modelling and inference for electrical capacitance tomography", *Measurement Science and Technology*, Vol. 20 No. 5, pp. 052002+, doi: 10.1088/0957-0233/20/5/052002, available at: http://dx.doi.org/10.1088/0957-0233/20/5/052002

Yang, W.Q. and Peng, L. (2003), "Image reconstruction algorithms for electrical capacitance tomography", *Meas. Sci. Technol*, Vol 14 No.1, pp. R1-R13.

Zang, L., Wang, H.X., Ma, M. and In, X.Z. (2006), "Image reconstruction algorithm for electrical capacitance tomography based on radial basis functions neural network", *Proceedings of the Fourth International Conference on Machine Learning and Cybernetics*, *Guangzhou*, pp. 4149-4152.

Zangl, H. and Neumayer, M. (2009), "Impact of leakage effects in electrical capacitance tomography due to short electrode length", *What, Where, When: Multidimensional Advances for Industrial Process Monitoring International Symposium*, *Leeds*.

Zangl, H., Watzenig, D., Steiner, G., Fuchs, A. and Wegleiter, H. (2007), "Non-iterative reconstruction for electrical tomography using optimal first and second order approximations", *Proceedings of the 5th World Congress on Industrial Process Tomography*, *Bergen*, pp. 216-223.

About the authors

Dr Hubert Zangl received the Dipl.Ing. degree in telematics, the Dr Tech. degree in Electrical Engineering, and the Venia Docendi for sensors and instrumentation from Graz University of Technology (TUG), Graz, Austria, in 2001, 2005, and 2009, respectively. From 2010 to 2013 he was an Associate Professor for Sensors and Instrumentation, Institute of Electrical Measurement and Measurement Signal Processing, TUG. Since September 2013 he is a Professor chairing Sensors and Actuators at the Institute of Smart System Technologies, Alpen-Adria-Universität Klagenfurt, Austria. He has authored or coauthored more than 100 international scientific publications. He is the holder of several patents His research interests focus on design and optimization of smart sensors and actuators, robustness and reliability of sensors and actuators, sensor signal processing, autarkic wireless sensors and energy harvesting. Dr Hubert Zangl is the corresponding author and can be contacted at: hubert.zangl@aau.at

Stephan Mühlbacher-Karrer received the Dipl.-Ing. degree, in telematics from the Graz University of Technology, Graz, Austria in 2012, where he focused on autonomous robots and telecommunications. He is currently pursuing the PhD degree at Alpen-Adria-Universität Klagenfurt, Klagenfurt, Austria, where he is a Research and Teaching Assistant with the Sensors and Actuators Group, Institute of Smart System-Technologies. His research interests include near field sensor technology, signal processing, and autonomous robots.